Carrier Capture Dynamics of Single InGaAs/GaAs Quantum-Dot Layers

K. N. Chauhan, D. M. Riffe,* E. A. Everett, D. J. Kim, and H. Yang†
Physics Department, Utah State University, Logan, UT 84322-4415

F. K. Shen
Center for Surface Analysis and Applications, Utah State University, Logan, UT 84322-4415
(Dated: May 22, 2013)

Using 800 nm, 25-fs pulses from a mode locked Ti:Al_2O_3 laser we have measured the ultrafast optical reflectivity of MBE-grown, single-layer $In_{0.4}Ga_{0.6}As$/GaAs quantum-dot (QD) samples. The QDs are formed via two-stage Stranski-Krastanov growth: following initial InGaAs deposition at a relatively low temperature, self assembly of the QDs occurs during a subsequent higher temperature anneal. The capture times for free carriers excited in the surrounding GaAs (barrier layer) are as short as 140 fs, indicating capture efficiencies for the InGaAs quantum layer approaching 1. The capture rates are positively correlated with initial InGaAs thickness and annealing temperature. With increasing excited carrier density the capture rate decreases; this slowing of the dynamics is attributed to Pauli state blocking within the InGaAs quantum layer.

I. INTRODUCTION

Due to both potential and realized photonics applications, carrier dynamics in self-assembled InGaAs/GaAs quantum dot (QD) systems have been the subject of numerous investigations. In the time domain the main tools for these investigations have been time resolved photoluminescence (PL) and time resolved pump-probe transmission measurements. (See, for example, Refs. 1–3.) In a typical experiment carriers in the surrounding GaAs barrier layers are initially excited. These carriers can then become captured by the InGaAs quantum layer (QL) [comprising the self-assembled QDs on top of a wetting layer (WL)], relax through states within the QL, and then recombine, often radiatively. Depending upon the details of the sample geometry, transport of the excited carriers within the barrier layer may be necessary before trapping by the QL can occur. These investigations have primarily focused on the relaxation of carriers within the QL system. The dynamics immediately after initial excitation – transport and capture – have been less thoroughly investigated.

The QD structures studied here are self assembled using a modified Stranski-Krastanov (SK) growth process (reviewed below).[4] Key to this process is the formation of QDs from an atomically flat (but strained) InGaAs layer during a high-temperature anneal of the sample. With this modified technique the QD morphology can be controlled not only via the amount of deposited InGaAs, but also through the annealing time and temperature. Various structures, including separated QDs, QD chains, and quantum dashes, have been formed using this process.[4,5]

With the ability to prepare distinct QD structures comes the potential to systematically investigate connections between QL morphology and carrier dynamics. In this paper we present results on carrier capture by the QL in three InGaAs/GaAs QD samples, all grown using modified SK self assembly. Our results show that the dynamics indeed depend upon the morphology: a thicker QL and a higher density and/or size of the dots results in faster capture by the quantum layer. Together with a diffusion model for carrier transport, our results further suggest that transport near the QL proceeds via ambipolar diffusion. Our experiments, carried out at relatively high excitation levels, also reveal the impact that state blocking has upon carrier dynamics in these QL systems.

II. SAMPLE AND EXPERIMENTAL DETAILS

The modified Stranski-Krastanov growth process has been previously described in detail;[4] we briefly review it here. After initial processing of the GaAs(100) substrate, a GaAs buffer layer (1300 to 2300 nm) is grown with the substrate held at ∼590 ° C. The sample is then cooled to a growth temperature (T_G) of 360 or 370 ° C, and approximately 10 or 15 monolayers (ML) of $In_{0.4}Ga_{0.6}As$ are grown. At this relatively low temperature the InGaAs layer remains atomically flat. The InGaAs QD's are then formed by heating the sample at a rate of 20 ° C/min under As flux to an annealing temperature (T_A) in the range 470 to 490 ° C; T_A is maintained for 120 s. The samples are then capped with ∼10 nm of GaAs before being removed from the growth chamber. The specific growth parameters for the samples studied here are shown in Table I. Reflection high-energy electron diffraction (RHEED) is used to determine the thickness of the initial InGaAs layer and also to monitor the formation of the QDs. As noted in Table I, the RHEED observations clearly indicated the formation of QDs on samples B and C, but not on sample A.

The QD morphology of other ∼10 ML samples grown in the same manner, but not capped, has been previously investigated with *in situ* scanning tunneling microscopy (STM).[4] The STM measurements reveal a QD density between 1.2 and 2.3 × 10^{11} cm^{-2}, with the typical QD having a base of ∼25 nm and a height of ∼8 nm. The morphology of the dots is sensitive to both the InGaAs growth and annealing temperatures. Notably, at higher annealing temperatures the dots align themselves

TABLE I. Sample growth parameters. Long sample designations (030907-1, e.g.) are for cross referencing to PL measurements.[6] Short designations (A, e.g.) are for internal reference in this paper. Also indicated are PL peak position λ_0 and line width $\delta\lambda$ for ground-state QD emission.

Sample	InGaAs (ML)	T_G ($^\circ$C)	T_A ($^\circ$C)	QDs via RHEED?	λ_0 (nm)	$\delta\lambda$ (nm)
030907-1 (A)	9.6	370	470	no	1080	110
030907-2 (B)	9.5	360	480	yes	1042	35
030607-2 (C)	14.6	370	490	yes	1085	55

in chains which, on average, lie along the $[1\bar{1}0]$ direction.

We have assessed the morphology of the capped samples studied here with *ex situ* atomic force microscopy (AFM); images of the samples are shown in Fig. 1. Although the thin GaAs cap obscures the finer features associated with the underlying QD structure, the AFM images clearly distinguish differences in QD morphology among the samples. Samples B and C exhibit structure that is most similar to the uncapped samples previous studied by STM: the dots are organized into chains, and the lateral density of the chains is similar to that of the uncapped samples. Conversely, the AFM image of sample A shows only a very low density ($\sim 10^9$ cm^{-2}) of features that can be associated with any formation of QDs; this sparseness of QDs is consistent with the dots not being observed with RHEED.

Low-temperature (3.6 K) photoluminescence data from (other pieces of) these samples have been previously obtained.[6] There are several features common to the PL spectra from all three samples: (i) a strong peak between 1040 and 1090 nm, (ii) a much weaker peak centered at 920 nm, and (iii) a tail that extends to ∼1450 nm. In addition, PL spectra from sample A exhibit a 980 nm peak. Based on comparisons with previously published luminescence spectra from other $In_{0.4}Ga_{0.6}As$/GaAs samples,[7–13] we assign the 1000 - 1100 nm peak to ground-state (GS) emission from the dots and the 920 peak to emission from the InGaAs wetting layer (WL) that remains below the dots after the high-temperature anneal. The PL wavelength of 920 nm from the WL indicates a WL thickness of 6 ML,[14,15] which is equal to the critical thickness for $In_{0.4}Ga_{0.6}As$/GaAs.[16] Also consistent with previously published PL measurements,[14,15] the wavelength of 980 nm from sample A is assigned to emission from regions of the InGaAs layer that did not form QDs, and so retain their original ∼10 ML thickness. The longer wavelength tail to 1450 nm is assigned to defect states in the vicinity of the InGaAs quantum layer (QL); these are likely interface states between the InGaAs and the GaAs cap. We have fit the QD GS peak to obtain both the peak position λ_0 and width $\delta\lambda$; the results of this analysis are shown in Table I.

The experimental setup for the ultrafast reflectivity measurements is similar to that for previous measurements on Si.[17] In the present experiment near-Gaussian pulses from a Ti:sapphire oscillator[18] (800 nm, 25 fs, 1.1 nJ) are split into a pump beam (at normal incidence) and an *s*-polarized probe beam (angle of incidence = 45°). The pump beam is chopped, and changes in the probe-beam reflectivity induced by the pump beam are measured as a function of time delay between the pump and probe pulses. The pump-pulse fluence is varied between ∼0.006 and ∼0.3 mJ/cm^2 using neutral density filters. Based upon the pump-pulse fluence and accounting for

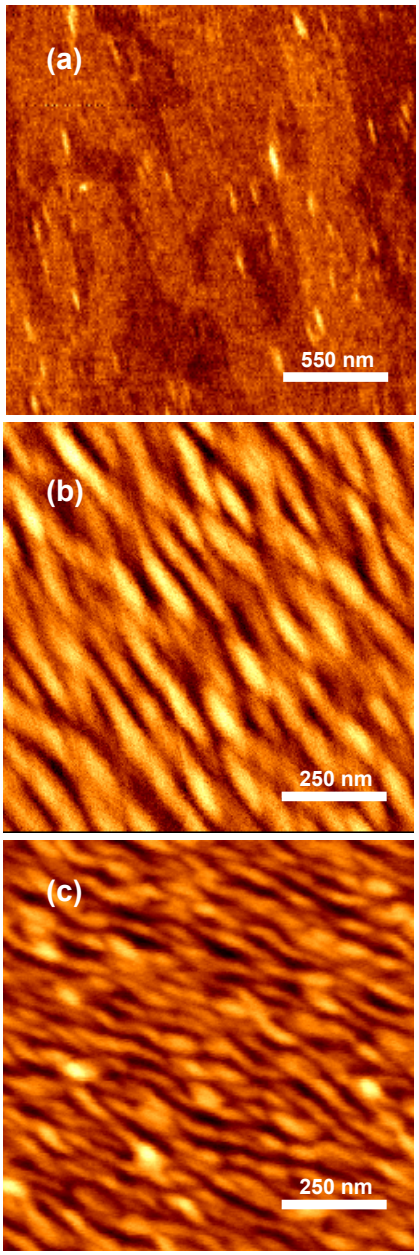

FIG. 1. (Color online) AFM images of the three samples in this study. Samples A, B, and C are shown in (a), (b), and (c), respectively. Image sizes are is 2.2 × 2.2 μm^2 for (a) and 1 × 1 μm^2 for (b) and (c).

saturation of the excited carriers at higher fluences,[19] we calculate the near-surface excited carrier density to range from 2.5×10^{17} cm^{-3} to 4.0×10^{18} cm^{-3} in our experiments.

III. RESULTS AND ANALYSIS

Typical reflectivity data are presented in Fig. 2(a), which shows data from all three samples at two different laser intensities. For all of the samples the initial reflectivity change is positive. For samples A and B this is followed by a monotonic decay back toward the initial reflectivity. For sample C the change in reflectivity becomes slightly negative before again becoming slightly positive. Even by 120 ps (our maximum time delay) the reflectivity of all of the samples has not yet fully recovered to its initial value. Given that PL lifetimes are typically several hundred ps for similar QD systems,[20,21] a lack of total recovery in the reflectivity even by 120 ps is not surprising. Referring to Table I and Fig. 2(a) (and noting that samples A and B have essentially identical amounts of deposited InGaAs), we see that the short-time decay rate is positively correlated with both annealing temperature T_A and the initial amount of InGaAs deposited and negatively correlated with the level of carrier excitation.

In order to quantitatively determine time constants associated with the reflectivity decay, we have analyzed the data using decaying exponential functions. Immediately after the reflectivity maximum the signal exhibits complexity that is not simply modeled. This is possibly related to the complex quantum-kinetic nature of GaAs carrier dynamics at the shortest time scales.[22,23] However, after a brief time (~250 fs) and up to at least several ps, the data can be described by a sum of two decaying exponentials (plus a nonzero background). The fitting reveals a dominant, positive-amplitude, faster-decay component for each reflectivity curve. For samples A and B the secondary, slower-decay component also has a positive amplitude. For sample C the secondary component has a negative amplitude. Typical fits of the reflectivity curves are illustrated in parts (b) and (c) of Fig. 2.

In Fig. 3 we plot the decay time τ_F of the faster component as a function of laser intensity for the three samples. As the graph indicates, at the lowest laser intensity in our study $\tau_F \approx 140$ fs for sample C while $\tau_F \approx 280$ fs for samples A and B. The figure shows for all three samples that τ_F monotonically increases with increasing laser intensity.

The slower-component relaxation time τ_S for samples A and B is also correlated with the pump-laser intensity. For sample B τ_S increases from ~2.5 ps at the lowest laser intensities to ~3.5 ps at maximum intensity. Similarly, for sample A τ_S varies from ~3 ps to ~6 ps as the intensity is increased. For sample C the longer time constant is ~9 ps; its variation versus excitation density is negligible.

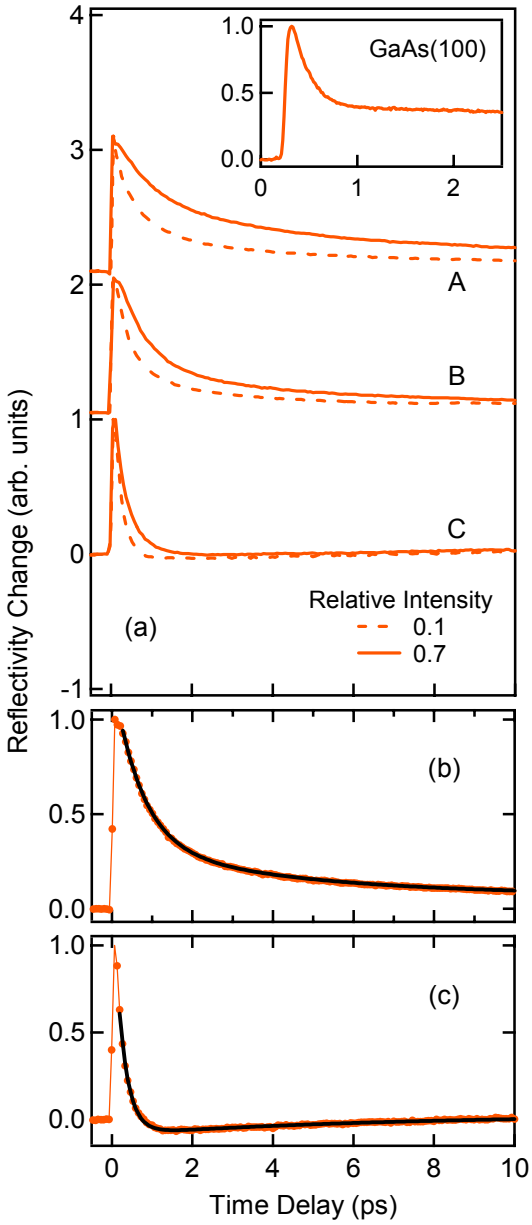

FIG. 2. (Color online) Reflectivity data vs time delay. Data from samples A, B, and C (as indicated) for two different pump intensities (values are relative to maximum intensity) are shown in (a). Data for A and B are vertically shifted for clarity. For comparison, reflectivity from GaAs(100) is shown in the inset of (a). Fits to reflectivity data are illustrated in (b) and (c) for samples B and C at a relative laser intensity of 0.7 and 0.34, respectively.

IV. DISCUSSION

A. Assignment of Decay Times

In the measurements on the QD samples the predominant effect of the pump pulse is to excite carriers from the valence band (VB) to the conduction band (CB)

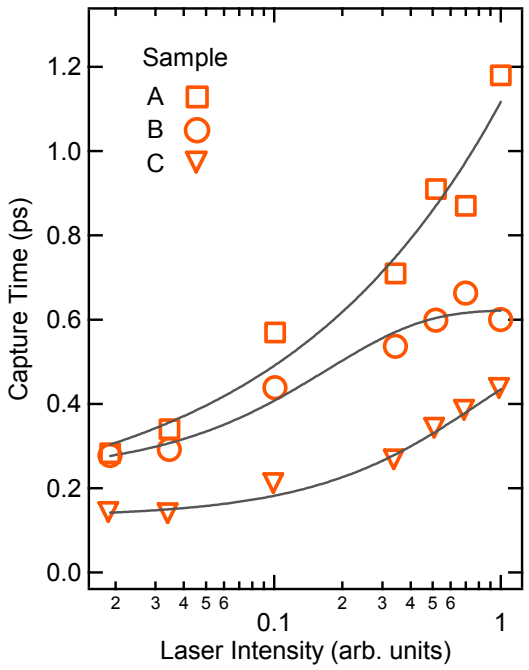

FIG. 3. (Color online) Fast capture time τ_F vs laser intensity for samples A, B, and C. Symbols are results of fitting the reflectivity data. Solid lines are guides to the eye.

in the GaAs that surrounds the InGaAs QL; in order to understand the ultrafast reflectivity from these samples it is instructive to first review carrier dynamics in GaAs and then consider the reflectivity of a standard GaAs(100) sample. Because reflectivity data at 800 nm are most sensitive to the CB electrons (as opposed to VB holes),[24] we concentrate on the electron dynamics. The pump pulse initially creates a CB electron distribution that can be characterized as having a degree of (quantum) coherence,[25,26] both anisotropic and isotropic momentum-space components,[27,28] and a nonthermal energy distribution.[22,23,29,30] Carrier-carrier and carrier-phonon scattering relaxes these components in several, approximately sequential, ways. (i) On a time scale of a few 10's of femtoseconds the coherence disappears and the anisotropic component relaxes, resulting in an isotropic, incoherent distribution in momentum space.[25–27] (ii) On a time scale of 100 to 200 fs the nonthermal energy distribution becomes thermalized, but still hot.[29–31] (iii) This distribution then cools close to the initial sample temperature on a time scale of a few ps.[32] (iv) On a much longer time scale the excited carriers eventually recombine across the gap, producing a fully equilibrated state.

Reflectivity data from a standard GaAs(100) sample is shown in the inset of Fig. 2(a). As with the QD samples, the initial reflectivity change is positive. For GaAs(100) the reflectivity then rapidly decays with a time constant of ∼150 fs. However, unlike the QD samples, the baseline for the fast decay is close to half of the initial reflectivity change. This baseline itself slowly decays (with a time constant of ∼20 ps) back to the initial reflectivity value. Also in contrast to the QD-sample data, the rate associated with the fast decay is (nearly) independent of the excitation intensity. Based on the results of GaAs carrier-dynamics studies, the 150 fs time constant can be associated with intracarrier thermalization of the initially excited electron distribution, while the 20 ps time constant can be associated with carrier recombination, most likely through surface recombination involving defects at the GaAs(100) surface.

We now consider the reflectivity of the QD samples. Because the initial reflectivity change of the QD samples is positive with a magnitude comparable to that of GaAs(100), we associate most of the reflectivity change in these samples with the excited electron population in the GaAs that surrounds the InGaAs QL. However, unlike the reflectivity data from GaAs(100), we cannot assign the fastest decay to intracarrier thermalization. The reasons for this are (i) the fast decay time varies significantly from sample to sample (∼140 fs for sample C to ∼280 fs for samples A and B at the lowest intensity, (ii) the decay time is a strong function of exciting laser intensity, and (iii) the baseline for the initial decay is much closer to zero than for GaAs(100). Because of these differences, and because the decay systematically varies with annealing temperature T_A and InGaAs growth thickness, we instead assign the decay to electron capture by the InGaAs QL.

As supported by results from a one-dimensional (1D) diffusion model (discussed below), we assign the faster decay time (τ_F) to the capture of electrons that are initially in the vicinity of the InGaAs QL. For samples A and B we assign the slower decay time (τ_S) to the capture of electrons that must diffuse into the region near the QL before becoming trapped, although there may also be a contribution to this time constant from intra-QL relaxation. Because the secondary-component amplitude for sample C is negative, it is unlikely to be associated with trapping; we thus assign this relaxation time to carrier relaxation within the QL.

The significance of the fast capture times can be assessed by a simple estimation of carrier transport in the vicinity of the QL. Because the reflectivity changes are most sensitive to changes in the sample index of refraction within an observation depth $d_{obs} = \lambda/(4\pi n) \approx 20$ nm of the surface (n is the GaAs index of refraction),[17] we first consider the transport and capture of carriers that lie within ±10 nm of the InGaAs QL. In our experiment the thermalized (but still hot) electrons have a temperature of ∼750 K,[33] which results in an average thermal-velocity component (perpendicular to the surface) of $\sim 3 \times 10^7$ cm/s. Thus, within (10 nm)/(3×10^7 cm/s) = 33 fs about half of the electrons within ±10 nm of the QL have interacted with the QL. This result suggests that electron capture by sample C (τ_F = 140 fs at the lowest intensities) is quite efficient.

B. 1D Diffusion Model

To gain further insight into the transport and capture process, we utilize a 1D diffusion model for the carrier density $N(z,t_D)$ (z = distance into the sample, t_D = time delay).[34] To keep the model as simple as possible we assume ambipolar diffusion, which is expected to be valid as long as electron and hole capture rates are not drastically different. Because (i) ambipolar diffusion is dominated by the holes and (ii) the excited hole temperature is close to RT, we use the RT ambipolar diffusion coefficient $D_a = 20$ cm^2/s.[35] The fate of a carrier incident on the QL is described using probabilities for capture, transmission, and reflection (c, t, and r, respectively; $1 = c+t+r$). These probabilities enter the model via capture and transmission velocities, which are related to the probabilities via $v_t = v_R t$ and $v_c = v_R c$, where $v_R = \sqrt{k_B T/2\pi m^*} \approx 1 \times 10^7$ cm/s is the Richardson velocity (m^* is the carrier effective mass).[36] Because recombination at the native-oxide surface of our GaAs(100) sample occurs on a timescale ≥ 20 ps, we simply assume that the carriers are perfectly reflected from the native-oxide surface of the QD samples.

Before presenting results obtained with the diffusion model, we acknowledge several potential pitfalls associated with a 1D diffusion model for describing transport in our QD samples. First, any diffusion model assumes that the carriers are described by a thermal distribution. This assumption is reasonable in the present case because intracarrier thermalization occurs with in ~150 fs. Second, the carrier mean-free path should be significantly smaller than the cap-layer thickness of 10 nm. The z-direction mean-free path is $l_z \approx 2v_R\tau_m$, where τ_m is the momentum relaxation time of the carriers. For a carrier density of 2×10^{17} cm^{-2}, $\tau_m = 40$ fs,[27] which yields $l_z = 8$ nm, closer to the cap-layer thickness than is ideal for modeling the transport strictly as diffusion. Third, it is clear from the AFM images in Fig. 1 that important lateral length scales for the cap are similar to its thickness, indicating that a 3D model is probably more appropriate. Given these last two issues, we expect any parameters extracted from the diffusion-model analysis to only be approximate in value. However, as we see below, with reasonable parameter values the 1D diffusion model does produce an approximately bi-exponential decay (in time) of the carrier density near the surface of the sample, consistent with the reflectivity data.

Using the model we have calculated $N(z,t_D)$ using the capture and transmission probabilities (c and t, respectively) as free parameters. In the experiment carrier excitation happens within several tens of fs, and so for simplicity the model is given an initial (excited) carrier density $N(z,0) = N_0 \exp(-z/\delta)$, where N_0 is the initial carrier density at the sample surface and $\delta = 670$ nm is the penetration depth of 800 nm light in GaAs.[37] This is the 0-ps curve shown in Fig. 4(a). As is observed for sample C, we are able to obtain a fast decay time of 0.14 ps for the near-surface carrier density for c varying between 0.8 and 0.7 and t concomitantly varying between 0 and 0.3. In parts (a) and (c) of Fig. 4 we show results for the combination $c = 0.77$ and $t = 0.1$. The curves in Fig. 4(a) illustrate the carrier density in the GaAs barrier layer for several times between 0 and 4 ps, while part (c) shows the (normalized) carrier density averaged over

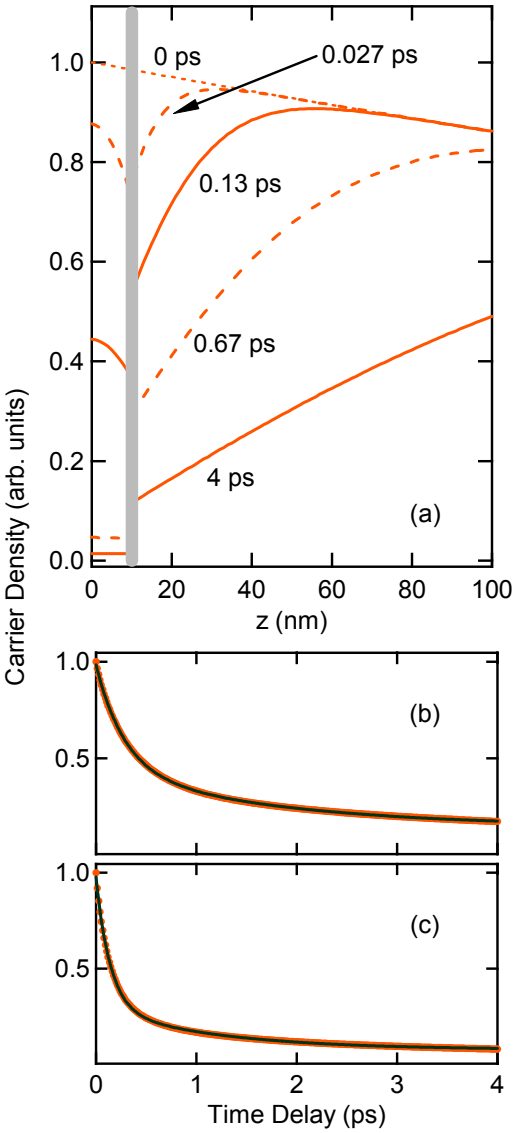

FIG. 4. (Color online) Results of 1D diffusion model. (a) Carrier density $N(z,t_D)$ vs distance z from sample surface at 5 different time delays t_D. The vertical line indicates location of QL. For this panel $t = 0.1$ and $c = 0.77$, which produces a fast decay similar to that of sample C at low excitation levels. (b) Near-surface (0 - 20 nm) carrier density vs time delay for $c = 0.3$ and $t = 0.1$, which gives decay similar to that of of samples A and B at low excitation level. Points are results of model; solid line is bi-exponential fit with with decay times of 0.28 and 1.6 ps. (c) Near-surface carrier density vs time delay for $c = 0.77$ and $t = 0.1$, as in (a). Solid-line fit has decay times of 0.14 and 1.1 ps.

the first 20 nm of the sample. A fit to the results in (c) indeed shows that the calculated decay is well approximated by a bi-exponential model with time constants of 0.14 and 1.2 ps. Part (b) of the figure illustrates model results for $c = 0.3$ and $t = 0.1$, which is well fit using time constants of 0.28 and 1.8 ps. This fast time constant matches the experimental result for samples A and B at low laser intensity. As expected, slower decay times (appropriate to higher excitations levels) correspond to even smaller capture probabilities. For example, an initial capture time of 1 ps can be obtained with c and t values of 0.05 and 0.1, respectively.

C. Capture Processes

Carrier capture by the QL can proceed via either carrier-phonon (cp) or carrier-carrier (cc) (i.e., Auger) scattering. For small carrier densities capture proceeds via cp scattering, but as the carrier density increases cc scattering becomes dominant, owing to the density dependence of the cc scattering rate. At our relatively high excitation densities (see details below), cc scattering is believed to be the primary capture mechanism.[38] We thus might expect to see the capture time τ_F decrease with increasing excitation level. However, we observe just the opposite, and so another process must be responsible for the behavior of τ_F with increasing carrier density.

We ascribe the increase in τ_F with excitation level to Pauli state blocking within the quantum layer.[39,40] This assessment comes from an estimation of the number of carriers captured (within the first several ps). First, at the lowest laser fluence ($\sim$0.006 mJ/cm^2) the initial near-surface carrier density $N_0 = 2.5 \times 10^{17}$ cm^{-3} corresponds to an areal density $N_0\delta = 1.7 \times 10^{13}$ cm^{-2}. From the diffusion model with parameters appropriate to sample C at the lowest laser intensity ($c = 0.77$ and $t = 0.1$, for example), we find that within 4 ps the carrier density captured by the InGaAs QL is $\sim 2 \times 10^{12}$ cm^{-2}. This corresponds to $\sim$10 carriers/QD. At the highest intensities where the excited carrier density is 4.0×10^{18} cm^{-3} and the capture time is between 0.4 and 1 ps, we calculate that on the order of 100 carriers/QD are captured by the QL within the first 4 ps. Such high carrier densities inhibit capture and relaxation within the QL via state blocking, and so it is no surprise that capture times increase with laser excitation. Further evidence that blocking is important comes from the second capture time τ_S for samples A and B, which also increases with laser intensity. In addition, the experimental values of τ_S are somewhat longer that those deduced from the diffusion model; this is also consistent with state blocking decreasing the capture probability c as carriers become trapped by the QL.

Comparisons of the τ_F curves vs laser intensity in Fig. 3 illuminates details of the impact that QL morphology has on the carrier dynamics. We first consider samples B and C, which had initial InGaAs-layers thicknesses of 9.5 and 14.6 ML, respectively. As evidenced from the AFM images and PL data, both samples comprise a high density of QD's sitting on top of a 6 ML WL, but because sample C contains a larger amount of InGaAs, we can surmise that the QDs on sample C are larger and/or more dense than those on sample B. A comparison of the the ground-state QD PL from samples B and C (see Table I), which occurs at slightly longer wavelength (λ_0) for sample C, suggests that the QDs on sample C are indeed larger than those on sample B. That the low-intensity values of τ_F are smaller for sample C thus suggests direct capture (from the GaAs barrier) by the QDs occurs in addition to capture via the WL. A comparison of τ_F for samples A and B is also enlightening. Recall that samples A and B contain essentially equal amounts of InGaAs, but substantially fewer QDs were formed on sample A, leaving a significant fraction of the InGaAs at its original thickness of 9.6 ML. Because the low-intensity values of τ_F are very close for these two samples we can conclude that capture by 9.6 ML of InGaAs is more efficient than capture by a 6 ML wetting layer, but direct capture by the QDs on sample B makes up for this difference. At higher excitation levels the τ_F values for sample A are significantly larger than those for sample B, consistent with QDs facilitating carrier relaxation within the InGaAs QL.

Our electron capture times are comparable to those in similar QL systems. (i) Using time resolved transmission, Norris and coworkers published a set of papers studying the carrier dynamics associated with $In_{0.4}Ga_{0.6}As/GaAs$ QDs (4 closely spaced QD layers, QD base $\sim$14 nm, height $\sim$7 nm, per layer density $\sim 5\times10^{10}$ cm^{-2}, WL thickness $\sim$7 ML).[3,41–43] Their excitation levels are typically less than one carrier per QD. While their work primarily focuses on intralayer dynamics, their modeling of these dynamics suggests a QL capture time of $\sim$0.5 ps,[43] comparable to our capture times. (ii) Liu et al. investigated carrier capture by InAs/GaAs QDs (QD base $\sim$30 nm, height $\sim$5 nm, density $\sim 4\times10^{10}$ cm^{-2}) using Ti:sapphire-laser based pump-probe reflectivity.[44] Their pump fluence ranged from $\sim$0.008 mJ/cm^2 (comparable to our lowest fluence) to $\sim$0.04 mJ/cm^2 (significantly below our maximum of $\sim$0.3 mJ/cm^2). Qualitatively, their reflectivity data are very similar to our data, as is their interpretation of those data. From their fitting they deduce an electron capture time that varies from 0.25 ps to 0.7 ps as the intensity is increased. They also attribute the increase in capture time versus excitation level to state blocking. (iii) Yarotski et al. also used time resolved reflectivity (800 - 875 nm) to study carrier dynamics in InAs/GaAS QDs (QD base $\sim$40 nm, height $\sim$3 nm, density $\sim 2.7\times10^{10}$ cm^{-2}, WL thickness $\sim$1.5 ML).[45] Their pump fluence (0.04 mJ/cm^2) was in the middle of our range of fluences. From their data they deduce an electron capture time of 0.5 ps for excitation (and probing) with 800 nm pulses. (iv) Lastly, Li et al. also used pump-probe reflectivity to investigate InAs/GaAs, both below and above the critical thickness ($\sim$1.7 ML) for forming InAs QDs.[46] For an InAs thickness of 1 ML their deduced

capture time shows a strong decrease from 4.5 to 0.6 ps as the incident fluence is increased from ∼0.001 to ∼0.01 mJ/cm^2. This strong decrease is consistent with cc scattering being responsible for the intensity dependence of their capture times. Apparently their excitation levels are below those where state filling begins to control the capture dynamics. We note that their highest intensity capture time of 0.6 ps is similar to capture times in our study and also that of Yarotski et al.[45] at similar fluences.

V. SUMMARY

With time-resolved pump-probe reflectivity we have investigated carrier dynamics in InGaAs/GaAs QD samples grown using two-stage SK self assembly. Specifically, we have determined electron capture times by these layers, which has provided insight into the influence that the QL morphology has on capture dynamics. Faster capture is facilitated by both a thicker WL and a higher density and/or larger size of the QDs. At high excitation levels state blocking within the QL is observed to hinder the capture process. In conjunction with a diffusion model of carrier transport in the barrier layer, our results are also consistent with ambipolar diffusion as playing the main role in carrier transport in the GaAs barriers near the QL. Inosfar as QL carrier capture is the first step in carrier relaxation and recombination in these systems, further investigation into the connections between morphology and dynamics in QLs fabricated by this novel growth process is warranted.

* Author to whom correspondence should be addressed; electronic mail: mark.riffe@usu.edu
† Current address: Nanoscience and Nanoengineering Program, South Dakota School of Mines and Technology, Rapid City, SD 57701

[1] S. Raymond, S. Fafard, P. Poole, A. Wojs, P. Hawrylak, S. Charbonneau, D. Leonard, R. Leon, P. Petroff, and J. Merz, Physical Review B **54**, 11548 (1996).
[2] B. Ohnesorge, M. Albrecht, J. Oshinowo, A. Forchel, and Y. Arakawa, Physical Review B **54**, 11532 (1996).
[3] T. Sosnowski, T. Norris, H. Jiang, J. Singh, K. Kamath, and P. Bhattacharya, Physical Review B **57**, 9423 (1998).
[4] D. J. Kim, E. A. Everett, and H. Yang, Journal of Applied Physics **101**, 106106 (2007).
[5] D. J. Kim and H. Yang, Nanotechnology **19**, 475601 (2008).
[6] A. M. Jones, Senior thesis, Brigham Young University (2010).
[7] K. Kamath, P. Bhattacharaya, T. Sosnowski, T. Norris, and J. Philips, Electronics Letters **32**, 1374 (1996).
[8] K. Kamath, N. Chervela, K. K. Linder, T. Sosnowski, H.-T. Jiang, T. Norris, J. Singh, and P. Bhattacharya, Applied Physics Letters **71**, 927 (1997).
[9] P. Bhattacharaya, S. Ghosh, S. Pradham, J. Singh, Z.-W. Wu, K. Kim, and T. Norris, IEEE Journal of Quantum Electronics **39**, 952 (2003).
[10] S. Fathpour, M. Holub, S. Chakrabarti, and P. Bhattacharaya, Electronics Letters **40**, 694 (2004).
[11] J. Cederberg, Journal of Crystal Growth **307**, 44 (2007).
[12] Y. I. Mazur, B. L. Liang, Z. M. Wang, D. Guzun, G. J. Salamo, G. G. Tarasov, and Z. Y. Zhuchenko, Journal of Applied Physics **100**, 054316 (2006).
[13] Y. I. Mazur, V. G. Dorogan, J. E. Marega, G. G. Tarasov, D. F. Cesar, V. Lopez-Richard, G. E. Marques, and G. J. Salamo, Applied Physics Letters **94**, 123112 (2009).
[14] M. Kudo and T. Mishima, Journal of Applied Physics **78**, 1685 (1995).
[15] V. Turck, F. Heinrichsdorff, M. Veit, R. Heitz, M. Grundmann, A. Krost, and D. Bimberg, Applied Surface Science **123/124**, 352 (1998).
[16] G. Sek, P. Poloczek, K. Ryczko, J. Misiewicz, A. Loffler, J. P. Reithmaier, and A. Forchel, Journal of Applied Physics **100**, 103529 (2006).
[17] A. J. Sabbah and D. M. Riffe, Phys. Rev. B **66**, 165217 (2002).
[18] D. M. Riffe and A. J. Sabbah, Review of Scientific Instruments **69**, 3099 (1998).
[19] A. V. Kuznetsov, C. S. Kim, and C. J. Stanton, Journal of Applied Physics **80**, 5899 (1996).
[20] G. Wang, S. Fafard, D. Leonard, J. E. Bowers, J. L. Merz, and P. M. Petroff, Applied Physics Letters **64**, 2815 (1994).
[21] L. Zhang, T. F. Boggess, D. G. Deppe, D. L. Huffaker, O. B. Shchekin, and C. Cao, Applied Physics Letters **76**, 1222 (2000).
[22] S. Bar-Ad, P. Kner, M. V. Marquezini, D. S. Chemla, and K. El Sayed, Phys. Rev. Lett. **77**, 3177 (1996).
[23] F. X. Camescasse, A. Alexandrou, D. Hulin, L. Bányai, D. B. Tran Thoai, and H. Haug, Phys. Rev. Lett. **77**, 5429 (1996).
[24] B. R. Bennett, R. A. Soref, and J. A. del Alamo, IEEE Journal of Quantum Electronics **26**, 113 (1990).
[25] P. C. Becker, H. L. Fragnito, C. H. B. Cruz, R. L. Fork, J. E. Cunningham, J. E. Henry, and C. V. Shank, Phys. Rev. Lett. **61**, 1647 (1988).
[26] W. A. Hügel, M. F. Heinrich, M. Wegener, Q. T. Vu, L. Bányai, and H. Haug, Phys. Rev. Lett. **83**, 3313 (1999).
[27] M. T. Portella, J.-Y. Bigot, R. W. Schoenlein, J. E. Cunningham, and C. V. Shank, Applied Physics Letters **60**, 2123 (1992).
[28] J. L. Oudar, A. Migus, D. Hulin, G. Grillon, J. Etchepare, and A. Antonetti, Phys. Rev. Lett. **53**, 384 (1984).
[29] J. Nunnenkamp, J. H. Collet, J. Klebniczki, J. Kuhl, and K. Ploog, Phys. Rev. B **43**, 14047 (1991).
[30] J. H. Collet, S. Hunsche, H. Heesel, and H. Kurz, Phys. Rev. B **50**, 10649 (1994).
[31] A. Alexandrou, V. Berger, and D. Hulin, Phys. Rev. B **52**, 4654 (1995).
[32] P. Langot, N. Del Fatti, D. Christofilos, R. Tommasi, and F. Vallée, Phys. Rev. B **54**, 14487 (1996).
[33] J. Shah, Solid-State Electronics **21**, 43 (1978).
[34] A. J. Sabbah and D. M. Riffe, Journal of Applied Physics **88**, 6954 (2000).
[35] J. F. Young and H. M. van Driel, Phys. Rev. B **26**, 2147 (1982).

[36] G. Bacher, C. Hartmann, H. Schweizer, T. Held, G. Mahler, and H. Nickel, Phys. Rev. B **47**, 9545 (1993).
[37] J. H. C. Casey, D. D. Sell, and K. W. Wecht, Journal of Applied Physics **46**, 250 (1975).
[38] A. V. Uskov, J. McInerney, F. Adler, H. Schweizer, and M. H. Pilkuhn, Applied Physics Letters **72**, 58 (1998).
[39] S. Lutgen, R. A. Kaindl, M. Woerner, T. Elsaesser, A. Hase, H. Künzel, M. Gulia, D. Meglio, and P. Lugli, Phys. Rev. Lett. **77**, 3657 (1996).
[40] T. Piwonski, I. O'Driscoll, J. Houlihan, G. Huyet, R. J. Manning, and A. V. Uskov, Applied Physics Letters **90**, 122108 (2007).
[41] J. Urayama, T. Norris, J. Singh, and P. Bhattacharya, Physical Review Letters **86**, 4930 (2001).
[42] J. Urayama, T. Norris, H. Jiang, J. Singh, and P. Bhattacharya, Applied Physics Letters **80**, 2162 (2002).
[43] J. Urayama, T. Norris, H. Jiang, J. Singh, and P. Bhattacharya, Physica B: Condensed Matter **316**, 74 (2002).
[44] H.-Y. Liu, Z.-M. Meng, Q.-F. Dai, L.-J. Wu, Q. Guo, W. Hu, S.-H. Liu, S. Lan, and T. Yang, Journal of Applied Physics **103**, 083121 (2008).
[45] D. A. Yarotski, R. D. Averitt, N. Negre, S. A. Crooker, A. J. Taylor, G. P. Donati, A. Stintz, L. F. Lester, and K. J. Malloy, J. Opt. Soc. Am. B **19**, 1480 (2002).
[46] Q. Li, Z. Y. Yu, and W. K. Ge, Solid State Communications **115**, 105 (2000).